Analysis of Chromatic Dispersion Induced Second Harmonic Distortions Including Semiconductor Laser Dynamics

K. H. Lee, H. Y. Choi, and W. Y. Choi
Department of Electrical and Electronic Engineering, Yonsei University
134 Shinchon-dong, Seodaemun-gu, Seoul 120-749, Korea
Tel:+82-2-2123-2874, Fax:+82-2-312-4584, E-mail: kyuk2@yonsei.ac.kr

Abstract

Investigating phase relationship of distortion caused by laser diode dynamics, we accurately modeled chromatic dispersion induced second harmonic distortion. We confirmed the results agree well with experiments in wide ranges of frequency and dispersion.

I. Introduction

There is a strong need for analog optical communication systems [1, 2]. The CATV and radio-on-fiber system are examples in which high frequency carriers and sub-carrier multiplexed data are simultaneously transmitted through a single fiber. In these systems, one of the key elements that determine the total system performance is optical source linearity. Direct modulation of semiconductor laser diodes is the simplest and most economical solution, but linearity of the laser diode is often not sufficient for many applications. Consequently, it is of significant importance to understand the causes for nonlinearity in laser diodes and analog optical links. In this paper, we present an accurate method for analyzing signal distortions due to laser diode nonlinearity and fiber dispersion especially in the systems using direct modulation and direct detection.

When laser diodes are directly modulated, there are several causes for nonlinearity. In sub-carrier multiplexed systems, which usually have many channels in the range of a few hundred MHz, static nonlinear L-I characteristics and clipping are the main causes for distortion. In highly dispersive media, chirp also causes large distortions [3, 4]. But in directly modulated systems, as light sources are not strictly monochromatic, laser diode dynamics and nonlinearities must be considered. For dynamic nonlinearity, which becomes more important as the modulation frequency increases, approximate [5, 6] distortion models have been reported. However, these approaches do not include distortions in frequency modulation and relative phase of nonlinear distortions compared to fundamental signal. So, it can not exactly describe the nonlinearity of directly modulated laser diode in a dispersive medium.

For a more accurate model of nonlinear distortions in analog optical links, we investigate nonlinear dynamics of laser diodes and include intrinsic dynamic distortion terms in analyzing chromatic dispersion induced distortions. Then, we confirm the results of our analysis with experimental measurement of second harmonic distortions in wide ranges of frequency and dispersion.

II. Dispersion induced distortion

For analyzing second harmonic distortions after fiber transmission, the E-field can be expressed as shown in Eq. (1) that fully considers laser diode dynamics [7]. However, the phase relationship, φ_{IM2}, φ_{FM1}, and φ_{FM2} relative to φ_{IM1} has not been investigated [7]. For accurate analysis of dispersion induced distortions, we investigated nonlinear dynamics of laser diode and determined magnitude and phase of each index.

$$E(t,z=0) \cong P_0^{1/2}(1+m_{IM1}\cos(\omega\cdot t+\varphi_{IM1})+m_{IM2}\cos(2\omega\cdot t+\varphi_{IM2}))^{1/2} \cdot \exp(\cdot m_{FM}\cos(\omega\cdot t+\varphi_{FM})+i\cdot m_{FM2}\cos(2\omega\cdot t+\varphi_{FM2})) \quad (1)$$

In order to model the influence of fiber dispersion, Meslener's numerical approach [3] is used including the relative phase of each fie ld component.

Electric field of the laser output in Eq. (1) can be expanded as shown below. Intensity modulation component is expanded in Fourier series and frequency modulation component in Bessel series. Then same frequency components are collected in C_n

$$\begin{aligned} E(t,z=0) &\cong P_0^{1/2}\Big(\sum_{n=-\infty}^{\infty} K_n\cdot e^{j\cdot n\omega\cdot t}\Big)\cdot\Big(\sum_{n=-\infty}^{\infty} J_n(m_{FM1})\cdot e^{j(n\cdot\omega\cdot t+n\varphi_{FM1})}\Big) \\ &\quad\cdot\Big(\sum_{n=-\infty}^{\infty} J_n(m_{FM2})\cdot e^{j(2n\omega\cdot t+n\varphi_{FM2})}\Big) \\ &\cong P_0^{1/2}\Big(\sum_{n=-\infty}^{\infty} C_n\cdot e^{j\cdot n\omega\cdot t}\Big) \end{aligned} \quad (2)$$

$$K_n=\int_T\frac{1}{T}(1+m_{IM1}\cos(\omega\cdot t+\varphi_{IM1})+m_{IM2}\cos(2\omega\cdot t+\varphi_{IM2}))^{1/2}\cdot e^{j\cdot n\omega t}dt \quad (3)$$

$$L_n=\sum_{l=-\infty}^{\infty} K_{n-l}\cdot J_l(m_{FM1})e^{j\cdot l\cdot\varphi_{FM1}} \quad (4)$$

$$C_n=\sum_{l=-\infty}^{\infty} J_l(m_{FM2})e^{j\varphi_{FM2}}\cdot L_{-2l+n} \quad (5)$$

In propagation through the fiber the different harmonics acquire different phase changes, $e^{jn^2\theta}$, due to fiber dispersion.

$$\theta = \frac{\lambda^2 \cdot D \cdot L \cdot \omega^2}{4\pi c} \tag{6}$$

Then detected photocurrent after fiber dispersion is obtained by squaring the electric field amplitude. Phase of each filed component is denoted $\varphi_n = \tan^{-1}\{\mathrm{Im}C_n)/\mathrm{Re}C_n)\}$.

$$\begin{aligned} I(t, z=L) &= \left|E(t, z=L)\right|^2 \\ &= \left(\sum_{n=-\infty}^{\infty} |C_n| e^{j(n\omega t + n^2\theta + \varphi_n)}\right)\left(\sum_{n=-\infty}^{\infty} |C_n| e^{-j(n\omega t + n^2\theta + \varphi_n)}\right) \end{aligned} \tag{7}$$

After squaring and gathering the same frequency components, fundamental frequency and second harmonic frequency can be expressed in Eq. (9) and (10) respectively.

$$\begin{aligned} F1 = &\{\sum_{n=-\infty}^{\infty} |C_n||C_{n+1}| \cos((2\cdot n+1)\theta + \varphi_{n+1} - \varphi_n)\} \cos\omega t \\ &+ \{\sum_{n=0}^{\infty} |C_n||C_{n+1}| \sin((2\cdot n+1)\theta + \varphi_{n+1} - \varphi_n) \\ &+ \sum_{n=-\infty}^{-1} -|C_n||C_{n+1}| \sin((2\cdot n+1)\theta + \varphi_{n+1} - \varphi_n)\} \sin\omega t \end{aligned} \tag{9}$$

$$\begin{aligned} F2 = &\{\sum_{n=-\infty}^{\infty} |C_n||C_{n+2}| \cos((4\cdot n+4)\theta + \varphi_{n+2} - \varphi_n)\} \cos 2\omega t \\ &+ \{\sum_{n=0}^{\infty} |C_n||C_{n+2}| \sin((4\cdot n+4)\theta + \varphi_{n+2} - \varphi_n) \\ &+ \sum_{n=-\infty}^{-1} -|C_n||C_{n+2}| \sin((4\cdot n+4)\theta + \varphi_{n+2} - \varphi_n)\} \sin 2\omega t \end{aligned} \tag{10}$$

III. Nonlinear dynamics of laser diode

To determine the each modulation index and phase in Eq. (1), we analyzed intrinsic nonlinear dynamics of semiconductor laser diode. Intrinsic dynamic nonlinearity in a laser diode is caused by the interaction between carriers and photons in laser cavity. This can be described based on the rate equations [8]. The rate equations used in our analysis are shown below.

$$\begin{aligned} \frac{dS(t)}{dt} &= \Gamma g_0 \frac{N(t)-N_t}{1+\varepsilon S(t)} S(t) - \frac{S(t)}{\tau_p} + \frac{\Gamma\beta}{\tau_n} N(t) \\ \frac{dN(t)}{dt} &= \frac{I(t)}{qV} - \frac{N(t)}{\tau_n} - g_0 \frac{N(t)-N_t}{1+\varepsilon S(t)} S(t) \\ \frac{d\phi(t)}{dt} &= \frac{\alpha}{2}[\Gamma g_0 (N(t)-N_t) - \frac{1}{\tau_p}] \\ \nu(t) &= \frac{1}{2\pi}\frac{d\phi(t)}{dt} \end{aligned} \tag{11}$$

S is photon density, N is carrier density, Γ is confinement factor, N_t is carrier density at transparency, τ_p is photon lifetime, τ_n is carrier lifetime, ε is gain compression factor, g_0 is gain slope, q is electron charge, V is volume of active region, and α is linewidth enhancement factor. Since any quantitative investigation based on the rate equations requires numerical values for the parameters used in equations, we extracted numerical values for the parameters of the laser used in our investigation following the procedure given in [9]. As we used commercial DFB laser diode and can extract a limited number of measurable parameters, we used modified rate equations as shown in Eq. (12) [9] and the resulting extracted parameters are shown in Table.1. P(t) is optical output power and X(t) is normalized carrier density. Other parameters are defined in Table 1.

$$\begin{aligned} \frac{dP(t)}{dt} &= \frac{B\tau_n I_{th}(X(t)-1) + 1/\tau_p}{1+FB\tau_p\tau_c P(t)} P(t) - \frac{P(t)}{\tau_p} \\ \frac{dX(t)}{dt} &= \frac{I(t)}{I_{th}\tau_n} - \frac{FB\tau_p(X(t)-1) + F/I_{th}\tau_n}{1+FB\tau_p\tau_c P(t)} P(t) - \frac{X(t)}{\tau_n} \\ \frac{d\phi(t)}{dt} &= \frac{\alpha}{2} B\tau_n I_{th}(X(t)-1) \end{aligned} \tag{12}$$

Parameters	Description	Dimension	Value
Ith	Threshold Current	mA	17.52
F=2qλ/hcη		A/W	12.56
Is	Spontaneous emission term	μA	12.59
B=Γg0/qV		GHz2/mA	176.34
K	K factor	ps	296.52
τn	Carrier Life Time	ns	0.179
α	Linewidth Enhancement Factor	-	3.09
τc=ε/g0		ps	3.18
τp	Photon Life Time	ps	4.33

Table.1. Extracted laser diode parameters

For the nonlinear distortion analysis, we used the perturbation method in which a sinusoidal input current of small magnitude with modulation frequency ω is assumed, and output photon density and carrier density have their harmonic responses varying around the mean values [8]. In equations, this can be expressed as following:

$$\begin{aligned} I(t) &= I_0 + \frac{1}{2}(\Delta I_1 e^{j\omega t} + \Delta I_1^* e^{-j\omega t}) \\ P(t) &= P_0 + \frac{1}{2}(\Delta P_1 e^{j\omega t} + \Delta P_1^* e^{-j\omega t}) + \frac{1}{2}(\Delta P_2 e^{j2\omega t} + \Delta P_2^* e^{-j2\omega t}) + \cdots \\ X(t) &= X_0 + \frac{1}{2}(\Delta X_1 e^{j\omega t} + \Delta X_1^* e^{-j\omega t}) + \frac{1}{2}(\Delta X_2 e^{j2\omega t} + \Delta X_2^* e^{-j2\omega t}) + \cdots \\ \Delta\nu(t) &= \nu_0 + \frac{1}{2}(\Delta\nu_1 e^{j\omega t} + \Delta\nu_1^* e^{-j\omega t}) + \frac{1}{2}(\Delta\nu_2 e^{j2\omega t} + \Delta\nu_2^* e^{-j2\omega t}) + \cdots \end{aligned} \tag{13}$$

Inserting Eq. (13) to Eq. (12), we can find relationships for first order terms as given in Eq. (14) and second order terms in Eq. (16). Each coefficient is

function of lower order terms and ω as shown in (15), (17) and (18).

$$\begin{aligned} &a_{11}\times\Delta P_1 + a_{12}\times\Delta X_1 = 0 \\ &a_{21}\times\Delta P_1 + a_{22}\times\Delta X_1 = \Delta I_1 \\ &\Delta v_1 = -a_{32}\times\Delta X_1 \end{aligned} \tag{14}$$

$$a_{11} = j\omega(1+FB\tau_p\tau_c P_0)+(B\tau_n I_{th}+2FB\tau_c P_0 - B\tau_n I_{th}X_0) - I_s I_{th} B\tau_n\tau_p\tau_c X_0$$

$$a_{12} = -(B\tau_n I_{th}P_0 + \frac{I_s I_{th} B\tau_n}{F} + I_s I_{th} B\tau_n\tau_p\tau_c P_0)$$

$$a_{21} = -(\frac{FB\tau_p\tau_c}{I_{th}\tau_n} I_0 - FB\tau_p X_0 + FB\tau_p - \frac{F}{I_{th}\tau_n} - \frac{FB\tau_p\tau_c}{\tau_n} X_0)/(\frac{1}{I_{th}\tau_n} + \frac{FB\tau_p\tau_c}{I_{th}\tau_n} P_0) \tag{15}$$

$$a_{22} = j\omega(1+FB\tau_p\tau_c P_0)+FB\tau_p P_0 + \frac{1}{\tau_n} + \frac{FB\tau_p\tau_c}{\tau_n} P_0)/(\frac{1}{I_{th}\tau_n} + \frac{FB\tau_p\tau_c}{I_{th}\tau_n} P_0)$$

$$a_{32} = -\frac{1}{2\pi 2}\frac{\alpha}{} B\tau_n I_{th}$$

$$\begin{aligned} &b_{11}\times\Delta P_2 + b_{12}\times\Delta X_2 = K_1 \\ &b_{21}\times\Delta P_2 + b_{22}\times\Delta X_2 = K_2 \\ &\Delta v_2 = -b_{32}\times\Delta X_2 \end{aligned} \tag{16}$$

$$K_1 = -j\omega\cdot FB\tau_p\tau_c\Delta P_1^2 + B\tau_n I_{th}\Delta X_1\Delta P_1 - FB\tau_c\Delta P_1^2 + I_s I_{th} B\tau_n\tau_p\tau_c\Delta X_1\Delta P_1 \tag{17}$$

$$K_2 = -j\omega\cdot FB\tau_p\tau_c\Delta X_1\Delta P + \frac{FB\tau_p\tau_c}{I_{th}\tau_n}\Delta I_1\Delta P_1 - FB\tau_p\Delta X_1\Delta P_1 - \frac{FB\tau_p\tau_c}{\tau_n}\Delta X_1\Delta P_1$$

$$b_{11} = j2\omega(1+FB\tau_p\tau_c P_0) - B\tau_n I_{th}X_0 + B\tau_n I_{th} + 2FB\tau_c P_0 - I_s I_{th} B\tau_n\tau_p\tau_c X_0)$$

$$b_{12} = -(B\tau_n I_{th}P_0 + \frac{I_s I_{th} B\tau_n}{F} + I_s I_{th} B\tau_n\tau_p\tau_c P_0) \tag{18}$$

$$b_{21} = -(\frac{FB\tau_p\tau_c}{I_{th}\tau_n} I_0 - FB\tau_p X_0 + FB\tau_p - \frac{F}{I_{th}\tau_n} - \frac{FB\tau_p\tau_c}{\tau_n} X_0)$$

$$b_{22} = j2\omega(1+FB\tau_p\tau_c P_0) + FB\tau_p P_0 + \frac{1}{\tau_n} + \frac{FB\tau_p\tau_c}{\tau_n} P_0)$$

$$b_{32} = -\frac{1}{2\pi 2}\frac{\alpha}{} B\tau_n I_{th}$$

From these equations, if we determine ΔI_1 as functions of ω, magnitudes and phases for all other terms can be obtained. For experimental verification, we determined ΔS_1 from measurements and used it as a reference to determine other term's magnitude and relative phase.

Values for both magnitude and phase indices can be obtained in Eq. (18). Real part and imaginary part of each term are simply noted as Re{} and Im{}.

$$\begin{aligned} &m_{IM1} = \Delta P_1 / P_0, \quad \varphi_{IM1} = \tan^{-1}(\mathrm{Im}(\Delta P_1)/\mathrm{Re}(\Delta P_1)) \\ &m_{IM2} = \Delta P_2 / P_0, \quad \varphi_{IM2} = \tan^{-1}(\mathrm{Im}(\Delta P_2)/\mathrm{Re}(\Delta P_2)) \\ &m_{FM1} = \Delta v_1 / f, \quad \varphi_{FM1} = \tan^{-1}(\mathrm{Im}(\Delta v_1)/\mathrm{Re}(\Delta v_1)) \\ &m_{FM2} = \Delta v_2 / 2f, \quad \varphi_{FM2} = \tan^{-1}(\mathrm{Im}(\Delta v_2)/\mathrm{Re}(\Delta v_2)) \end{aligned} \tag{18}$$

Each index is shown in Fig. 1 and compared with the simulation results. Analytically induced results matched well with numerically simulated results. Second harmonic modulation indices, m_{IM2} and m_{FM2}, are enhanced in half the resonance frequency. This result is in accordance with other previously reported results [8].

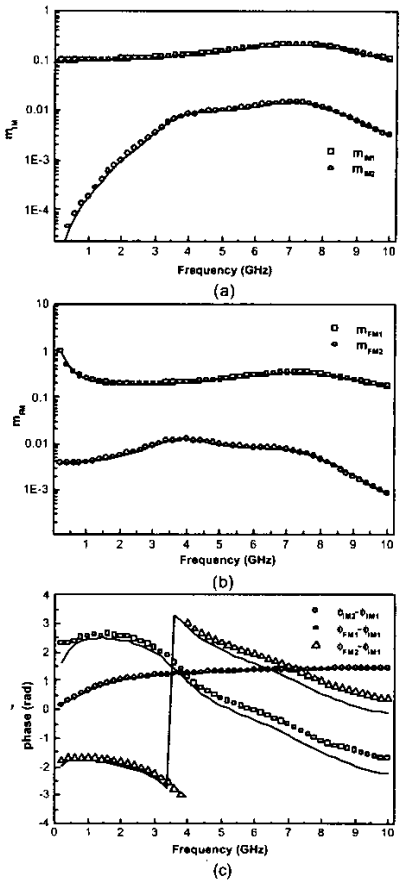

Fig.1 Simulation results (dots) and analytical results (line): (a) Intensity modulation index: m_{IM1} and m_{IM2}, (b) Frequency modulation index: m_{FM1} and m_{FM2}, (c) Phase relations of modulation indices normalized to ϕ_{IM1}.

IV. Experimental verification

Experiments are performed in order to verify the accuracy of our model. Fig.2 is experimental setup for measuring the signal and second harmonic distortion varying transmission distance. We made back reflection effect negligible using fiber pig-tailed DFB LD with isolator. We also confirmed nonlinearity of receiver is below -70dBc. Compensating fiber loss with EDFA and attenuator we observed second harmonic distortion caused by intrinsic dynamics of laser diode and fiber dispersion. For a fixed link length (40km) with varying modulation frequencies and at a fixed modulation frequency (2GHz & 4GHz) for varying fiber lengths experiments are performed. In Fig. 3, dots show

measured fundamental signals and second harmonic distortions.

Calculated results with our model are shown in solid lines. When we calculate modulation indices in part III using the results of II, we used measured ΔP_1 instead of ΔI_1 as reference. Because ΔI_1 is current injected in active region, we are able to bypass the package effects. Good agreement with the measured results can be seen. For comparison, calculated results with previously reported models are shown in dashed [3, 4] and dash-dotted lines [5, 6] respectively. Dashed line is the results when the laser diode output is assumed to be monochromatic. And dash-dotted line is the results when distortion in frequency modulation is neglected. As shown in fig.3, as modulation frequency increase, laser dynamic effects increase and become dominant around half the resonance frequency. Thus, other previously reported results shows difference with simulation results increasing the fiber length and modulation frequency. But our analytic results matched well and accurate modeling for directly modulated laser diode is possible for the entire frequency ranges and transmission distances.

V. Conclusions

We analyzed the nonlinear distortions of the directly modulated laser diodes that can be used in analog optical links. For the accurate distortion model, intrinsic dynamic distortion is considered. From rate equation, relative phase relation of distortion and signal is obtained and exact description of optical field is constructed. We believe the results of our investigation will be useful for realizing simple analog optical links that are based on the directly modulated laser diodes.

References

[1]. R. Olshansky, *et al.*, , *J. of Lightwave Technol.*, vol. 7, no. 9, pp. 1329-1342, Sept. 1989.

[2]. J. C. Fan, *et al.*, *IEEE Trans. Microwave Theory and Tech.*, vol. 45, no. 8, pp. 1390-1397, 1990.

[3]. G. J. Meslener, *IEEE J. of Quantum Electron.*, vol. 20, no.10, pp. 1208-1216, 1984.

[4]. C. S. Ih, *et al.*, *IEEE J. of Selected Areas in Commun.*, vol. 8, no. 7, pp. 1296-1303, 1990.

[5]. H. T. Lin, *et al.*, *J. of Lightwave Technol.* vol. 14, no. 11, pp. 2567-2574, 1996.

[6]. C. Y. Kuo, *J. of Lightwave Technol.* vol. 10, no. 2, pp. 235-243, 1992

[7]. Eva Peral, *et al.*, *J. of Lightwave Technol.*, vol 18, no. 1, pp.84-89, 2000

[8]. J. L. Bihan, *et al.*, *IEEE J. of Quantum Electron.*, vol.40, no. 4, pp. 899-903, 1994

[9]. L. Bjerkan, *et al.*, *J. of Lightwave Technol.*, vol. 14, no. 5, pp. 839-850, 1996.

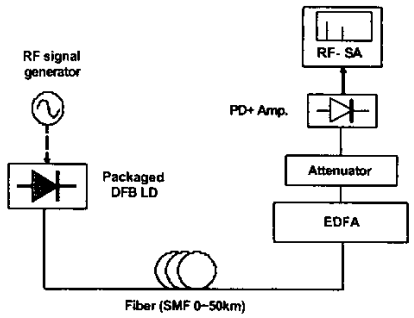

Fig.2 Experimental setup

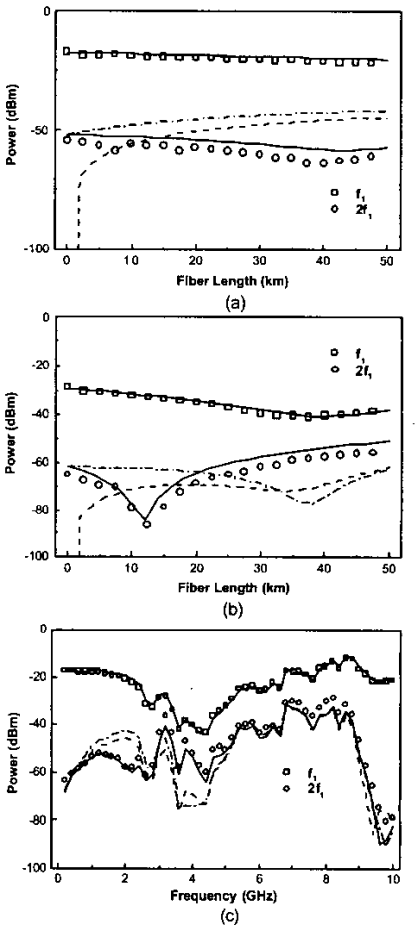

Fig.3 Experimental results (dots) and analytical results (line): fundamental signal @GHz (a) and 4GHz (b)) and second harmonic distortion along the SMF (0~50km), after 40km (c)